Catal Lett (2009) 129:259–265
DOI 10.1007/s10562-008-9806-9

Palladium and Molybdenum Mono and Bimetallic Catalysts on Modernite for Direct NO Decomposition Reaction

Rodrigo S. da Silveira · Andréa M. de Oliveira · Sibele B. C. Pergher · Victor Teixeira da Silva · Ione M. Baibich

Received: 3 October 2008 / Accepted: 25 November 2008 / Published online: 8 January 2009

Abstract Palladium and/or molybdenum catalysts supported on mordenite were prepared and characterized by XRD, UV–vis, DRS, textural properties analysis, TPR, TPD and chemical analysis. The Mo-catalyst rapidly deactivated after the first minutes reaction. The Pd-catalysts were active in the NO decomposition reactions. The incorporation of Mo in the Pd-catalysts improved their catalytic properties.

Keywords NO decomposition · Palladium catalysts · Molybdenum catalysts · Mordenite

1 Introduction

Energy conversion processes that use high temperatures are responsible for the production of the pollutant nitrogen oxide gases in the atmosphere. These gases are noxious since they give rise to ozone layer degradation, acid rain, and photochemical smog and are one of the causative agents of the greenhouse effect [1–3].

Due to the environmental issues caused by NO_x release in the atmosphere, interest in the development of technologies aimed at decreasing NO_x emissions is growing [4–6]. The selective reduction of NO_x using CO [7], CH_4 [8] and C_3H_6 [9] as reducting agents, and the direct NO decomposition reaction [10–14], represent a suitable alternative for the decomposition of these contaminant gases; in particular the direct NO decomposition since the process does not require a reducing agent. After the finding that a Cu-ZSM-5 catalyst was able to directly decompose NO, the study of different metals and supports has expanded with the ultimate goal of understanding and improving the catalytic performance [6, 10].

Zeolites are crystalline aluminosilicates that present a high surface area, adsorption capability, tridimensional framework of micro- and mesoporous and a possibility of impregnation of dispersed metallic cations. Therefore, these materials have been extensively used as inorganic supports for heterogeneous catalysts [15–17]. In particular, mordenite is a promising support due to its unique properties such as acidity, unidirectional porous geometry and thermal and hydrothermal stability [8, 13, 14]. This zeolite has been used as support for Pd catalyst in the NO selective reduction of NO with CH_4 [18]. It is worth mentioning that Pd is not only active for NO_x reduction, but also for CO and hydrocarbons oxidation. In previous works, we have prepared mono- and bimetallic palladium catalysts using different materials as supports such as alumina [19], MCM-41 [11, 12] and zeolite NaY [20]. Furthermore, we have studied mordenite as a support for Pd and Cu catalysts [13, 14]. These preliminary results showed that mordenite acts as a promoter maintaining the catalyst active for longer time and being more selective than the other used supports.

In this work, mono- and bimetallic palladium and molybdenum catalysts supported on mordenite were prepared using $Pd(NO_3)_2$ and $[Mo(CO)_6]$ as precursors. The photochemical activation of molybdenum hexacarbonyl

R. S. da Silveira · A. M. de Oliveira · I. M. Baibich (✉)
Instituto de Química, Universidade Federal do Rio Grande do Sul, CP 15003, Porto Alegre, RS 91501970, Brazil
e-mail: ione@iq.ufrgs.br

S. B. C. Pergher
Departamento de Química, Universidade Regional Integrada do Alto Uruguai e das Missões, Campus Erechim, Brazil

V. T. da Silva
Núcleo de Catálise, Programa de Engenharia Química, Universidade Federal do Rio de Janeiro, Rio de Janeiro, RJ, Brazil

generates species [$Mo(CO)_{6-n}$] that can be incorporated more effectively on the support without risking of metal oxidation [19]. The materials were characterized by X-ray diffraction spectroscopy (XRD), textural analysis, UV–vis by diffuse reflectance spectroscopy (DRS-UV), temperature programmed reduction (TPR) and chemical analysis by inductively coupled *plasma*-optical emission *spectroscopy* (ICP-EOS) and tested in the direct decomposition of NO.

2 Experimental

2.1 Catalysts Preparation

The used support was a commercial mordenite CBV-10A (Si/Al = 7.0) in the Na form provided by the Instituto de Tecnologia Quimica, Valence, Spain. Prior to its use, the mordenite was treated in a synthetic airflow following a temperature program, which consisted of raising the temperature from room temperature to 673 K at a heating rate of 5 K min^{-1}. Intermediate 1 h steps at 423 and 573 K were used before the final desired temperature was reached.

Palladium was incorporated in the pre-treated mordenite (3 g) by ionic exchange with a solution of $Pd(NO_3)_2$ 0.8 mmol L^{-1} at 323 K during 36 h. The material was filtered, washed with deionized water, dried at 373 K for 24 h and calcinated at 673 K under a flow of synthetic air for 5 h, according to method adapted from Aylor et al. [21]. Two palladium catalysts were obtained following this method: $Pd_{0.8}$MOR [$Pd(NO_3)_2$ 0.8 mmol L^{-1}] and $Pd_{1.9}$MOR [$Pd(NO_3)_2$ 5 mmol L^{-1}].

Molybdenum incorporation was carried out through photochemical activation of the organometallic compound [$Mo(CO)_6$] (Aldrich) dissolved in hexane in the presence of the support or PdMOR. The quantities used were 3.0 g of support, 1.666 g of [$Mo(CO)_6$] and 50 mL of hexane.

The photochemical reactions were performed at room temperature under an Ar atmosphere using a Philips HPL-N (125 W) UV lamp fitted into a Pyrex cold finger. In order to monitor the reaction progress, small liquid samples were withdrawn for analysis by FTIR where the decrease in the γ(CO) band intensity was monitored. After irradiation, the solid was filtered and washed with hexane. Finally, the generated subcarbonyl species were decomposed by thermal treatment under H_2 at 573 K for 3 h. The resulting catalysts were labeled as $Mo_{0.8}$MOR (molybdenum incorporated directly into the mordenite support), $Pd_{0.8}Mo_{0.6}$MOR (molybdenum incorporated on PdMOR) and $Mo_{0.3}Pd_{1.9}$MOR [firstly Mo incorporation, followed by the thermal treatments of activation and reduction, and ionic exchange with 5 mmol L^{-1} of $Pd(NO_3)_2$]. The subscript numbers denote the metal content.

2.2 Catalysts Characterizations

X-ray diffraction patterns were obtained on a Siemens D 5,000 operated at 40 kV and 25 mA with radiation from a Cu target ($\lambda = 1.5403$ Å) in the range $2° < 2\theta < 65°$. The stepsize was 0.02 and a steptime of 1 s was employed. Chemical analysis was performed by ICP-OES using a Perkin-Elmer Optima 2000 DV instrument.

The specific surface area of the solids, which were prior degassed at 623 K for 12 h, under vacuum, was determined by the BET (Brunauer, Emmett and Teller) multipoint method on a Gemini Micromeritics apparatus, using nitrogen as the probe. The porous size distribution was obtained using the BJH (Barret, Joyner and Halenda) method. The TPR experiments were carried out in a conventional apparatus. The samples were pre-heated at 673 K (5 K min^{-1}) in flowing Ar (30 mL min^{-1}) for 1 h. They were then reduced at 773 K (10 K min^{-1}) under a flow of 1.74% H_2/Ar (30 mL min^{-1}). Following reduction, the samples were purged with Ar for 1 h at 773 K.

TPD of adsorbed NO was carried out in a microreactor coupled to a quadrupole mass spectrometer (Prisma, Balzers). A Quadstar analytical system was used for selecting and recording different signal intensities of masses as a function of the temperature. In a typical experiment, the catalyst sample was first submitted to thermal treatment under a flow of synthetic air (20 mL min^{-1}) from room temperature up to 673 K and holding the final temperature for 5 h. The temperature was dropped to room temperature and the gas flowing throughout the reactor was changed from synthetic air to pure H_2 (30 mL min^{-1}) and the temperature raised again up to 573 K at a heating rate of 10 K min^{-1}, holding the final temperature for 2 h. The adsorption of NO was performed by introducing pulses of 1% NO in helium (AGA S.A > 99%) until saturation. After adsorption, the catalyst sample was heated at 10 K min^{-1} to 773 K in flowing helium (50 mL min^{-1}), holding the final temperature for 1 h.

UV-Diffuse reflectance spectra (DRS) of samples were recorded in the 200–800 nm range with a Cary 500 Spectrophotometer, using $BaSO_4$ as a reference. The references for the experiments were the catalyst supports.

2.3 Catalytic Tests

Catalytic evaluations with NO were carried out in a fixed-bed quartz reactor. Prior to reaction, the catalysts were activated with synthetic air (20 mL min^{-1}) at 673 K for 5 h and reduced in situ at 573 K for 2 h. The NO decomposition reaction was studied firstly as a function of temperature in the range 623–773 K and as a function of time at 673 K using a feed mixture containing 500 ppm of NO in an argon background. The flow rate was adjusted

to 72.5 cm^3 min^{-1} with a space velocity of 15,000 h^{-1}. The effluent gases were analyzed by an FTIR MB100-BOMEM Spectrometer equipped with a multiple reflection gas cell (7.0 m path length and 2.1 L volume). The NO, NO_2 and N_2O stretching bands at 1,955–1,790 cm^{-1}, 1,658–1,565 cm^{-1} and 2,266–2,159 cm^{-1} respectively, were monitored. In order to calculate the NO conversions from the IR data, a method of treating the measured absorbance values was used to determine the NO concentration at the entrance of the gas IR cell (reactor exit) [22].

3 Results and Discussion

Chemical analysis and specific surface area values for the catalysts are presented in Table 1. The metal loads results found in the solid after incorporation, were measured by ICP-OES. These metal contents are those used in the catalysts nomenclature. Table 1 shows that the monometallic palladium catalysts had a specific surface area values close to that of the support. On the other hand, catalysts $Mo_{0.8}$MOR and $Pd_{0.8}Mo_{0.6}$MOR, with higher molybdenum content, presented a slight decrease in the specific surface area (S_g) and pore volume values in comparison with the mordenite support, thus suggesting that the presence of molybdenum led to a some extent of porous blockage and consequent decrease in these values.

The sample $Mo_{0.3}Pd_{1.9}$MOR, incorporated less Mo than the other samples even using the same [$Mo(CO)_6$] concentrations. This catalyst did not show a significant reduction in specific area probably as a consequence of the low Mo loading. Since Mo was incorporated first and the sample was submitted to thermal treatment before Pd impregnation, it is possible that some Mo leaching has occurred.

The XRD patterns (not shown here) of the samples indicate that mordenite structure was maintained after the metals incorporations.

UV-DRS spectra of the catalysts are shown in Fig. 1. It can be seen that $Pd_{0.8}$MOR spectrum displays weak bands in the region of 400 nm, that can be attributed to Pd d-d transitions and at 280 nm due to the metal—oxygen charge transfer [23, 24]. The same bands in the $Pd_{1.9}$MOR and $Mo_{0.3}Pd_{1.9}$MOR spectra are more intense, pointing to higher metal content in this sample.

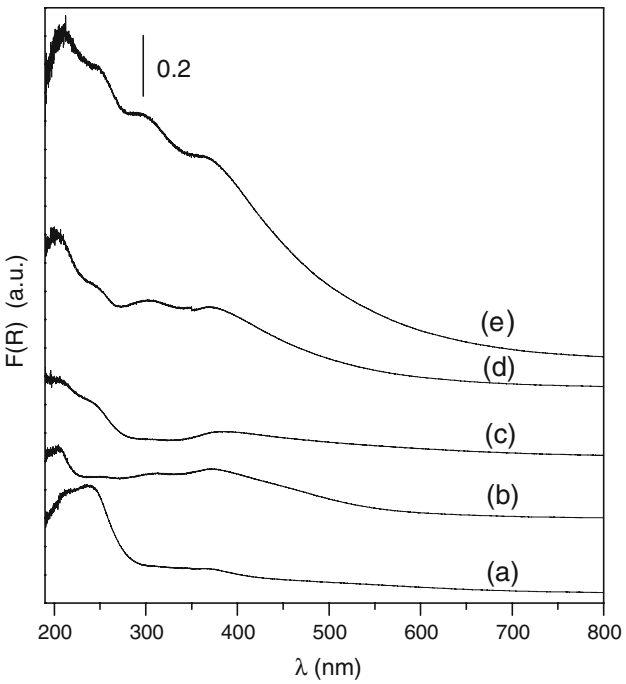

Fig. 1 DRS-UV spectra for (**a**) $Mo_{0.8}$MOR, (**b**) $Pd_{0.8}$MOR, (**c**) $Pd_{0.8}Mo_{0.6}$MOR, (**d**) $Pd_{1.9}$MOR and (**e**) $Mo_{0.3}Pd_{1.9}$MOR

The monometallic catalyst $Mo_{0.8}$MOR displays bands in the region 200–250 nm attributed to molybdenum species in a tetrahedral coordination mode [25]. The bands related to Mo oxide particles which are commonly located in the 290–330 nm region are not observed [7, 24], meaning that octahedral coordinated molybdenum species are not present in this sample. This result suggests that the incorporation process and the metal load led to well disperse molybdenum on the support. We observed in the spectrum of the catalyst $Pd_{0.8}Mo_{0.6}$MOR (Fig. 1c) that not only the bands in the 280–330 nm region, but also those located at 400 nm are less intense than those observed for the monometallic catalysts $Mo_{0.8}$MOR and $Pd_{0.8}$MOR. However, in Fig. 1c, a shoulder located at around 280 nm which can be attributed to tetrahedrally coordinated molybdenum can be seen, indicating that in this sample molybdenum is also in a high dispersion state on the support.

Table 1 Results of chemical analysis, specific surface area and pore volume for the support and the catalysts

Materials	%Pd[a] (wt)	%Mo[a] (wt)	%Al[a] (wt)	Specific surface area (m^2/g)[b]	Pore volume (cm^3/g)[b]
Mordenite	–	–	–	358	0.21
$Mo_{0.8}$MOR	–	0.83	4.80	314	0.19
$Pd_{0.8}$MOR	0.81	–	4.47	364	0.21
$Pd_{1.9}$MOR	1.9	–	3.30	360	0.21
$Pd_{0.8}Mo_{0.6}$MOR	0.88	0.65	4.33	330	0.19
$Mo_{0.3}Pd_{1.9}$MOR	1.94	0.31	4.82	347	0.21

[a] By ICP-OES

[b] By BET, BJH

Catalyst $Mo_{0.3}Pd_{1.9}$MOR presents a spectrum (Fig. 1e) different in intensity to that of $Pd_{0.8}Mo_{0.6}$MOR (Fig. 1c). In fact, since the molybdenum content is lower in $Mo_{0.3}Pd_{1.9}$MOR, all of the observed bands might be due to palladium, which is in higher content. However, since the catalyst $Pd_{1.9}$MOR presents the same amount of palladium than that of the catalyst $Mo_{0.3}Pd_{1.9}$MOR, the difference in intensity between the two spectra reflects an interaction between the two metals.

The TPR profiles of the catalysts are shown in Fig. 2. The catalyst $Pd_{1.9}$MOR did not present any peak (not shown in the Figure) in the temperature range studied.

Monometallic Pd catalysts on zeolites present reduction peaks at low temperatures and frequently a second peak at higher temperatures up to 700 K depending on the support, due to species located in the cavities. On the other hand, molybdenum catalysts present reduction peaks at higher temperatures up to 900 K depending on the species found on the support [26]. Conversely to $Pd_{1.9}$MOR, for $Pd_{0.8}$MOR, a reduction peak at 298 K, a negative peak at 333 K due to a β-hydride palladium phase decomposition and a third peak at 360 K attributed to Pd^{2+} ions that interact with oxygen of the support crystal lattice were observed [27].

The $Mo_{0.8}$MOR profile shows a large reduction peak at 873 K due to MoO_3 reduction [28, 29]. In the $Mo_{0.3}Pd_{1.9}$MOR profile, the negative peak due to the β-hydride palladium phase decomposition was observed. The peak at 395 K is due to Pd^{2+} that interacts with oxygen of the crystal lattice. The peaks at higher temperatures (623–723 K) can be attributed to molybdenum species or might reflect an interaction between the two metals.

It is worth noting the difference in the Pd reduction of the two catalysts $Pd_{1.9}$MOR and $Mo_{0.3}Pd_{1.9}$MOR. In the former (not shown in the Figure) the reduction probably happens at lower temperature, since no peaks were observed over the temperature range studied. This indicates that large palladium oxide particles were formed, leading to a weaker interaction with the support and consequently to a lower temperature of reduction. On the other hand, the TPR profile of $Mo_{0.3}Pd_{1.9}$MOR, shows the presence of peaks that might be due to palladium species interacting more strongly with the support or interacting with molybdenum atoms. This result suggests that the previous molybdenum incorporation on the support promoted this strong interaction.

In Fig. 3 the results of NO temperature desorption are shown for the catalysts $Mo_{0.8}$MOR, $Pd_{0.8}Mo_{0.6}$MOR and $Pd_{0.8}$MOR. The $Mo_{0.8}$MOR profile (Fig. 3a) shows a NO desorption peak at low temperatures and a less intense one at 650 K. However, significant amounts of N_2 and N_2O were not observed on the temperature range studied. In the monometallic Pd catalyst (Fig. 3b) it is observed a NO peak desorption at low temperature and a weak one at around 550 K. This catalyst also displays N_2 and N_2O desorption in the range 373–473 K. These peaks confirm that palladium has an important role in the NO dissociation on the catalyst surface [30]. Comparing the TPD profiles

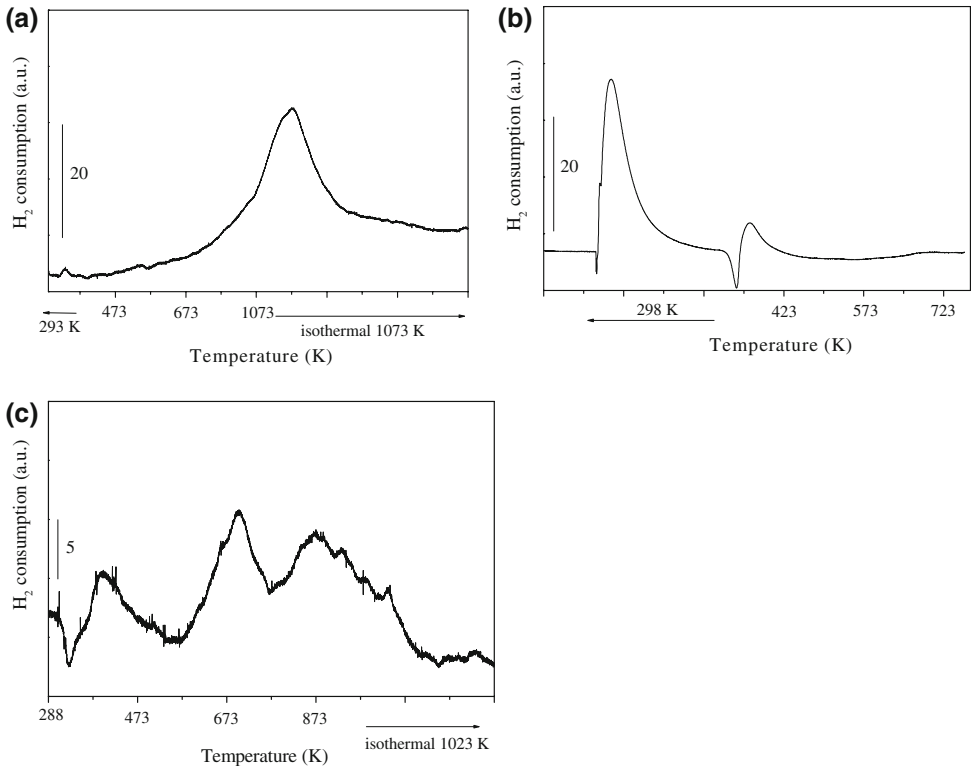

Fig. 2 TPR profile of (**a**) $Mo_{0.8}$MOR, (**b**) $Pd_{0.8}$MOR (**c**) $Mo_{0.3}Pd_{1.9}$MOR

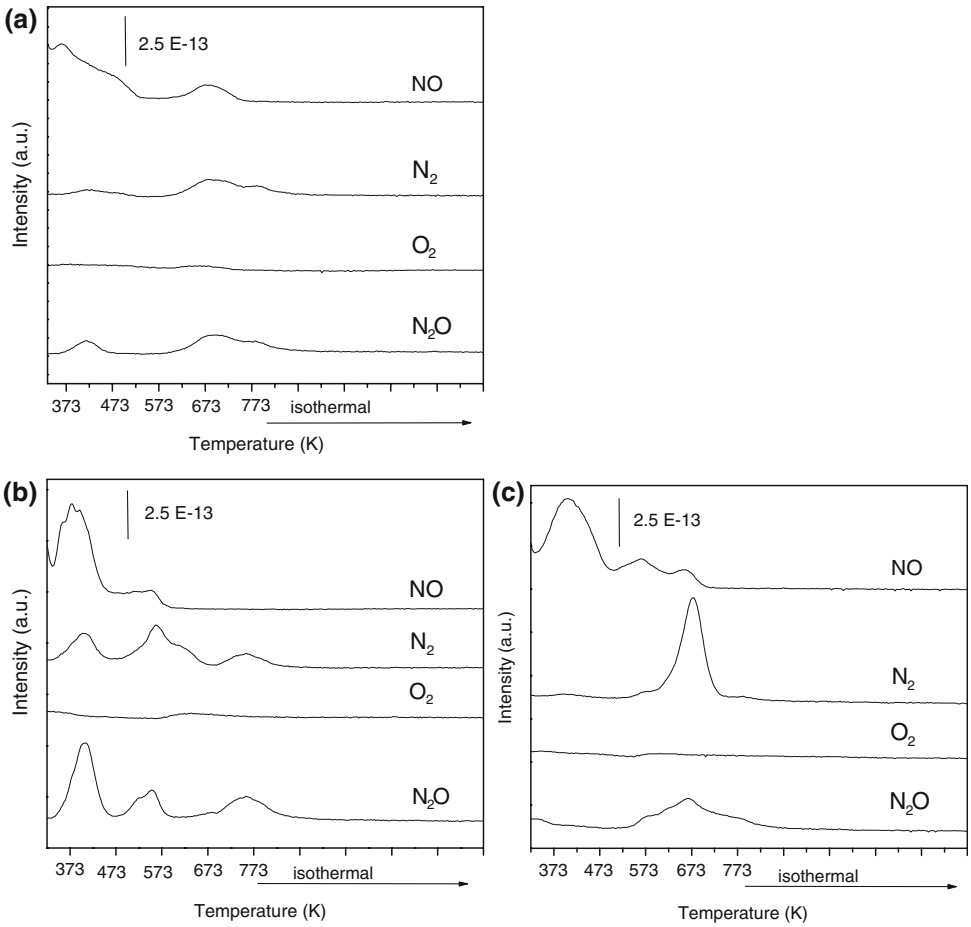

Fig. 3 NO TPD of the catalysts (**a**) $Mo_{0.8}MOR$, (**b**) $Pd_{0.8}MOR$, (**c**) $Pd_{0.8}Mo_{0.6}MOR$

for $Pd_{0.8}Mo_{0.6}MOR$ (Fig. 3c) and the Pd monometallic one a difference between the peaks of N_2 and N_2O can be noted. They occur over one temperature range leading to more N_2 than N_2O and consequently reflecting more selectivity in this catalyst.

In Fig. 4 the catalytic tests for the NO decomposition reaction of the catalysts are shown. The reaction temperature chosen was 673 K because gave the best results. In all reactions NO_2 production was not detected. Figure 4a shows the NO conversion with time. The catalyst

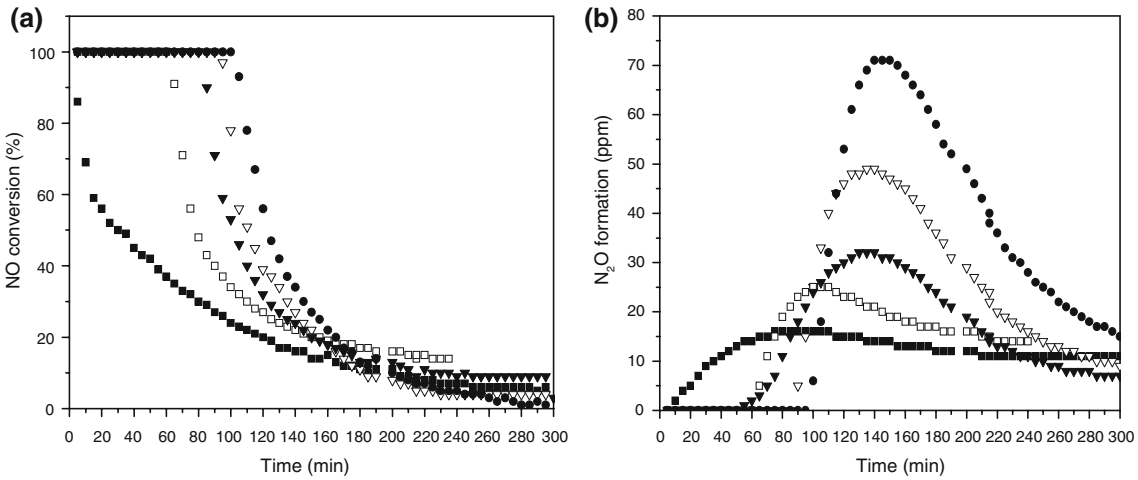

Fig. 4 (**a**) NO conversion (%) and (**b**) N_2O formation (ppm) versus time of reaction for (■)$Mo_{0.8}MOR$, (▽)$Pd_{0.8}MOR$, (▼)$Pd_{0.8}Mo_{0.6}MOR$, (□)$Pd_{1.9}MOR$ and (●)$Mo_{0.3}Pd_{1.9}MOR$ at 673 K

$Mo_{0.8}$MOR looses its activity rapidly and does not present activity after 250 min. If the catalysts $Pd_{1.9}$MOR and $Mo_{0.3}Pd_{1.9}$MOR are compared, Fig. 4a shows that the bimetallic one remains at 100% conversion for a longer period of time than the monometallic catalyst with the same Pd content. This suggests that the prior incorporation of molybdenum has a positive effect upon the activity. On the other hand, $Pd_{0.8}$MOR and $Pd_{0.8}Mo_{0.6}$MOR had similar conversion times at 100%, but the bimetallic one presented higher residual activity (after 200 min reaction). It is interesting to observe also that the monometallic catalyst $Pd_{0.8}$MOR, with a lower Pd load, spent a longer time at 100% conversion than the one with higher Pd content, $Pd_{1.9}$MOR. This result could probably be attributed to differences in the Pd particle size. The TPR results for $Pd_{0.8}$MOR show peaks at higher temperature that are not seen for $Pd_{1.9}$MOR. The catalyst deactivations observed could be attributed to oxidation of the Pd active sites by the oxygen atoms originated from the NO decomposition reaction and remaining adsorbed on the surface. This is in agreement with the NO TPD results (Fig. 3) where no oxygen molecules were detected.

In Fig. 4b the N_2O production with reaction time is shown, which gives indirectly the catalyst selectivity to N_2 and O_2. Comparing the catalysts $Pd_{1.9}$MOR and $Mo_{0.3}Pd_{1.9}$MOR, it can be seen that the bimetallic analog slows down by 30 min the N_2O formation, but the amount formed was higher than with the monometallic analog. On the other hand, if $Pd_{0.8}$MOR and $Pd_{0.8}Mo_{0.6}$MOR are compared, it can be seen that the presence of Mo produced N_2O in lower quantity, in accord with the TPD profiles found (Fig. 3). The selectivity and TPD results indicate that the monometallic catalysts led to $NO \rightarrow N_2 + N_2O$ mainly, as it is known for Pd catalysts on alumina [19]. Comparing with previous work on NaY [20], mordenite catalysts has analogous activities than the catalyst supported on NaY (1.26% Pd prepared by dry impregnation) but better selectivities to N_2 and O_2, since the selectivities to N_2O were lower than in the NaY catalyst. The role of Mo was related previously to the metal capability of adsorbing and dissociating NO [12]. In this work, this second metal acts in a different way in the two catalysts: when this metal is present in lower amounts and was incorporated before Pd, the activity of the catalyst increases but not the selectivity. On the contrary, when Mo is present in higher contents and incorporated after Pd, it doesn't contribute to improve the activity, but leads to a better selectivity.

4 Conclusions

Crystallinity values found from XRD show that the mordenite structure was maintained after the metal incorporation processes, reflecting that the preparation procedures were suitable. The monometallic Pd catalyst with less metal content $Pd_{0.8}$MOR presented a stronger interaction with the support as was suggested by TPR and catalytic tests results. This effect might be responsible for its higher activity when compared with the $Pd_{1.9}$MOR. The presence of molybdenum led to better residual activities (activities after 250 min) and for $Pd_{0.8}Mo_{0.6}$MOR to better selectivity to N_2.

Acknowledgments To the Brazilian agencies CNPq, Fapergs and COPESUL for financial support, to M. A. S. Baldanza for TPD measurements and to Dr. John Spencer (University of Greenwich, England) for proofreading this article.

References

1. Kustova MYu, Rasmussen SB, Kustov AL, Christensen CH (2006) Appl Catal B 67:60
2. Tonetto GM, Ferreira ML, Damiani DE (2003) J Mol Catal A 193:121
3. Dallago RM (2001) Ph.D. Thesis. Universidade Federal do Rio Grande do Sul, Brazil
4. Busca G, Larrubia MA, Arrighi L, Ramis G (2005) Catal Today 107:139
5. Pârvulescu VI, Grange P, Delmon B (1998) Catal Today 46:233
6. Armor JN (1995) Catal Today 26:99
7. Schmal M, Baldanza MAS, Vannice MA (1999) J Catal 185:138
8. Ohtsuka H, Tabata T (1999) Appl Catal B 21:133
9. Meunier FC, Ukropec R, Stapleton C, Ross JRH (2001) Appl Catal B 30:163
10. Kustova MYu, Kustov A, Christiansen SE, Leth KT, Rasmussen SB, Christensen CH (2006) Catal Commun 7:705
11. Cónsul JMD, Peralta CA, Benvenutti EV, Ruiz JAC, Pastore HO, Baibich IM (2006) J Mol Catal A 246:33
12. Cónsul JMD, Costilla I, Gigola CE, Baibich IM (2008) Appl Catal A (in press)
13. de Oliveira AM, Crizel LE, da Silveira RS, Pergher SBC, Baibich IM (2007) Catal Commun 8:1293
14. De Oliveira AM, Baibich IM, Machado NRCF, Mignoni ML, Pergher SBC (2008) Catal Today (in press)
15. Corma A (2003) J Catal 216:298
16. Li M, Yeom Y, Weitz E, Sachtler WMH (2005) J Catal 235:201
17. Giannetto GP (1990) Zeolitas: Caracteristicas. Propriedades Y Aplicaciones Industriales, EdiT, Caracas
18. Pieterse JAZ, Booneveld S (2007) Appl Catal B 73:327
19. Sica AM, dos Santos JHZ, Baibich IM, Gigola CE (1999) J Mol Catal A 137:287
20. Pergher SBC, Dallago RM, Veses RC, Gigola CE, Baibich IM (2004) J Mol Catal A 209:107
21. Aylor AW, Lobree LJ, Reimer JA, Bell AT (1997) J Catal 172:453
22. Dallago RM, Schifino J, Baibich IM, Veses RC (2004) Can J Anal Sci Spectr 49:78
23. Feio LSF, Hori CE, Damyanova S, Noronha FB, Cassinelli WH, Marques CMP, Bueno JMC (2007) Appl Catal A 316:107
24. Córdoba LF, Flytzani-Stephanopoulos M, de Correa CM (2001) Appl Catal B 33:25
25. Duan A, Wan G, Zhao Z, Xu C, Zheng Y, Zhang Y, Dou T, Bao X, Chung K (2007) Catal Today 119:13
26. Jones A, McNicol B (1986) Temperature-programmed reduction characterization. Marcel Dekker, New York

27. Zina MS, Ghorbel A (2004) Solid State Sci 6:973
28. Grzechowiak JR, Mrozinska K, Masalska A, Góralski J, Rynkowski J, Tylus W (2006) Catal Today 114:272
29. Song Y, Sun C, Shen W, Lin L (2007) Appl Catal A 317:266
30. Cordatos H, Gorte RJ (1996) J Catal 159:112